Performance Evaluation of Cruise-Controlled Vehicles on a Macroscopic Scale

Dionysis Theodosis, Iasson Karafyllis, George Titakis, Ioannis Papamichail, and Markos Papageorgiou *Life Fellow, IEEE*

***Abstract*— In this paper, we study the performance of a class of cruise-controllers for automated vehicles on a macroscopic scale. We first show that the solution of the corresponding second-order macroscopic model can be approximated by the solution of a nonlinear heat-type equation. To study the behavior induced on the macroscopic model by the first-order approximation, we derive a conservative finite-difference scheme that respects the corresponding entropy conditions. Finally, a traffic simulation scenario and a comparison with the Lighthill-Witham-Richards (LWR) model are given, illustrating the benefits of the use of cruise-controlled vehicles.**

I. INTRODUCTION

Macroscopic traffic flow models have been widely used as they are able to capture the collective behavior of vehicles in a traffic stream and can express certain relationships between traffic flow, density and mean speed. Macroscopic traffic flow models can be in general distinguished between first-order models, governed by the continuity equation, and second-order models where the continuity equation is coupled with the momentum equation (see [2], [9], [16], [21], [27]).

In [11], the design of cruise controllers for automated vehicles lead to a second-order traffic flow model with several fluid-like characteristics. Our main objective now, is to evaluate the performace of the cruise controllers on a macroscopic scale and compare it with that of human driven vehicles. To that end, we require an efficient numerical scheme to obtain an approximation of the solution of the macroscopic model. It is shown first that the solutions of the second-order macroscopic model can be approximated by the solutions of a first-order equation. The corresponding equation is a nonlinear heat-type equation, whose diffusion/viscosity coefficient depends on both the density and the spatial derivative of the density (see also [8], [14], [15]), a feature that is rarely studied in the literature where typically the diffusion coefficient exclusively depends on the density, see for instance [19], [20], [22], [23] and references therein. Furthermore, inspired by the mechanical energy of the original second-order system, certain functionals are defined, providing entropy-like conditions that characterize physically meaningful solutions, see [7], [24].

Several finite-difference methods have been proposed to study a variety of nonlinear heat equations, see for instance [3], [5], [6], [10], and references therein. In this paper, we propose an explicit finite-difference scheme that, in addition to being conservative (Proposition 1), it also respects the corresponding entropy conditions (Proposition 2 and Proposition 5). Moreover, a condition on the step size is provided that is an nonlinear version of the Courant-Friedrichs-Levy condition (Proposition 3). To demonstrate the properties of the solutions of the nonlinear heat equation and evaluate the performance of automated vehicles using the controllers of [11], we present a realistic traffic simulation scenario showing that the mean flow produced by automated vehicles is much higher than that of the LWR (see [16], [21]).

The structure of the paper is as follows. Section II is devoted to the presentation of a second-order traffic flow model and the approximation of its solution by the solution of a particular nonlinear heat equation. Section III presents the proposed numerical scheme and its properties. Section IV presents a numerical example. Finally, some concluding remarks are given in Section V.

Due to space constraints, the proofs of all results can be found in [25], which also contains certain links between the numerical solution and the weak solution of the nonlinear heat equation.

Notation. Throughout this paper, we adopt the following notation. $\mathbb{R}_+ := [0, +\infty)$ denotes the set of non-negative real numbers. Let $A \subseteq \mathbb{R}^n$ be an open set. By $C^0(A; \Omega)$, we denote the class of continuous functions on $A \subseteq \mathbb{R}^n$, which take values in $\Omega \subseteq \mathbb{R}^m$. By $C^k(A; \Omega)$, where $k \geq 1$ is an integer, we denote the class of functions on $A \subseteq \mathbb{R}^n$ with continuous derivatives of order k, which take values in $\Omega \subseteq \mathbb{R}^m$. When $\Omega = \mathbb{R}$ the we write $C^0(A)$ or $C^k(A)$. Let $I \subseteq \mathbb{R}$ be a given interval. For $p \in [1, \infty)$, $L^p(I)$ denotes the set of equivalence classes of Lebesgue measurable functions $f : I \to \mathbb{R}$ with $\|f\|_p := \left(\int_I |f(x)|^p dx\right)^{1/p} < +\infty$. $L^\infty(I)$ denotes the set of equivalence classes of measurable functions $f : I \to \mathbb{R}$ for which $\|f\|_\infty = \operatorname{ess\,sup}_{x \in I} (|f(x)|) < +\infty$. Let $u : \mathbb{R}_+ \times \mathbb{R} \to \mathbb{R}$, $(t, x) \to u(t, x)$ be any function differentiable with respect to its arguments. We use the notation $u_t(t, x) = \frac{\partial u}{\partial t}(t, x)$ and $u_x(t, x) = \frac{\partial u}{\partial x}(t, x)$ for the partial derivatives of u with respect to t and x, respectively. We use the notation $u[t]$ to denote the profile at certain $t \geq 0$, $(u[t])[x] := u(t, x)$, for all $x \in \mathbb{R}$.

The research leading to these results has received funding from the European Research Council under the European Union's Horizon 2020 Research and Innovation programme/ ERC Grant Agreement n. [833915], project TrafficFluid.

I. Karafyllis is with the Dept. of Mathematics, National Technical University of Athens, Zografou Campus, 15780, Athens, Greece. D. Theodosis, G. Titakis, I. Papamichail, and M. Papageorgious are with Dynamic Systems and Simulation Laboratory, Technical University of Crete, Chania, 73100, Greece. M. Papageorgiou is also with the Faculty of Maritime and Transportation, Ningbo University, Ningbo, China.

II. A NONLINEAR HEAT EQUATION

A. Motivation and Derivation of a Nonlinear Heat Equation

In the recent paper [11], the study of microscopic vehicle movement control laws (cruise controllers) for autonomous vehicles on lane-free roads brought forth the following macroscopic model that holds for $\tau > 0$, $\xi \in \mathbb{R}$:

$$\tilde{\rho}_\tau + (\tilde{\rho}\tilde{v})_\xi = 0 \tag{1}$$

$$\begin{aligned}\tilde{\rho}\tilde{q}(\tilde{v})\tilde{v}_\tau + \tilde{\rho}\tilde{q}(\tilde{v})\tilde{v}\tilde{v}_\xi + \tilde{P}'(\tilde{\rho})\tilde{\rho}_\xi = (\tilde{\mu}(\tilde{\rho})\tilde{g}'(\tilde{v})\tilde{v}_\xi)_\xi \\ - \tilde{\rho}\tilde{f}(\tilde{v} - v^*)\end{aligned} \tag{2}$$

with constraints $\tilde{\rho}(\tau,\xi) \in [0, \rho_{max})$, $\tilde{v}(\tau,\xi) \in (0, v_{max})$ for $\tau > 0$, $\xi \in \mathbb{R}$, where $\rho_{max} > 0$, $v_{max} > 0$, and $v^* \in (0, v_{\max})$ are constants. The states $\tilde{\rho}(\tau,\xi)$, $\tilde{v}(\tau,\xi)$ are the traffic density and mean speed, respectively, at time $\tau > 0$ and position $\xi \in \mathbb{R}$ on a highway, while the constants $\rho_{max} > 0$, $v_{max} > 0$, and $v^* \in (0, v_{\max})$ are the maximum density, the maximum speed, and the speed set-point, respectively. Moreover, $\tilde{f} : \mathbb{R} \to \mathbb{R}$ is a C^1 function with $\tilde{f}(0) = 0$ and $\xi\tilde{f}(\xi) > 0$ for all $\xi \neq 0$, $\tilde{g} \in C^1(\mathbb{R})$ is an increasing function with $\tilde{g}'(\tilde{v}) > 0$ for all $\tilde{v} \in \mathbb{R}$ and $\tilde{q}(\tilde{v})$ is defined by

$$\tilde{q}(\tilde{v}) = v_{max}^2 \frac{v_{max}\tilde{v} - 2\tilde{v}v^* + v^* v_{max}}{2(v_{max} - \tilde{v})^2\tilde{v}^2} \tag{3}$$

Model (1), (2) is a fluid-like model where the term $\tilde{P}'(\tilde{\rho})\tilde{\rho}_\xi$ is a pressure term and expresses the tendency to accelerate or to decelerate based on the (local) density; while the term $(\tilde{\mu}(\tilde{\rho})\tilde{g}'(\tilde{v})\tilde{v}_\xi)_\xi$, is a viscosity term, by analogy with the theory of fluids, with $\tilde{\mu}(\tilde{\rho})$ playing the role of dynamic viscosity, see [12], [17]. The functions $\tilde{\mu} : [0, \rho_{\max}) \to \mathbb{R}_+$, $\tilde{P} : [0, \rho_{max}) \to \mathbb{R}_+$ are $C^1([0, \rho_{max}))$ and satisfy the following properties

$$\lim_{\tilde{\rho} \to \rho_{max}^-} \tilde{P}(\tilde{\rho}) = +\infty \tag{4}$$

$$\begin{aligned}&\tilde{\mu}(\tilde{\rho}) = 0,\ \tilde{P}(\tilde{\rho}) = 0 \text{ for all } \tilde{\rho} \in [0, \bar{\rho}], \text{ and} \\ &\tilde{\mu}(\tilde{\rho}) > 0,\ \tilde{P}(\tilde{\rho}) > 0 \text{ for all } \tilde{\rho} \in (1, R)\end{aligned} \tag{5}$$

where the constant $\bar{\rho} \in (0, \rho_{max})$ is referred to as the interaction density due to the fact that for all $\rho \in [0, \bar{\rho}]$ there is no interaction among the vehicles (see (5)). The term $f(\tilde{v} - v^*)$ is a *relaxation term* that describes the tendency of vehicles to adjust their speed to the given speed set-point $v^* \in (0, v_{\max})$.

Remarks: (i) Model (1), (2) has certain characteristics from the kinematic theory of fluids. Traffic flow is isotropic, as in fluid flow, since vehicles react to both downstream and upstream vehicles.

(ii) There are infinite equilibrium points, namely the points where $\tilde{v}(\xi) \equiv v^*$ and $\tilde{\rho}(\xi) \leq \bar{\rho}$ for all $\xi \in \mathbb{R}$.

(iii) The selection of $\tilde{\mu}(\tilde{\rho})$, $\tilde{g}(\tilde{\rho})$ has several implications on the characteristics for the traffic flow. The dynamic viscosity $\tilde{\mu}(\tilde{\rho})$ makes the "traffic fluid" act as a Newtonian fluid. However, in contrast to actual fluids, the dynamic viscosity also satisfies (5). For isentropic (or barotropic) flow of gases, the dynamic viscosity and the pressure are always increasing functions of the fluid density (see the discussion in [12]).

Model (1), (2) is to be studied under the following conditions for all $\tau \geq 0$:

$$\lim_{\xi \to \pm\infty} \tilde{\rho}(\tau,\xi) = 0 \tag{6}$$

$$\lim_{\xi \to \pm\infty} \tilde{v}(\tau,\xi) = v^* \tag{7}$$

$$\int_{-\infty}^{+\infty} \tilde{\rho}(\tau,\xi)d\xi < +\infty. \tag{8}$$

Condition (6) expresses the fact that "far downstream and far upstream" the highway is "empty", i.e., there are no vehicles. Condition (8) expresses the fact that the total mass of the vehicles in the highway is finite. Let $r \in \mathbb{R}$ be a given constant length. Using the variable transformation $\xi = rx + v^*\tau$, $x \in \mathbb{R}$ and the dimensionless quantities $\tau = \frac{r}{v^*}t$, $b = \frac{v_{max} - v^*}{v^*}$, $R = \frac{\rho_{max}}{\bar{\rho}}$, $w = \frac{\tilde{v} - v^*}{v^*}$, $\rho = \frac{\tilde{\rho}}{\bar{\rho}}$, we obtain the following dimensionless model for $t > 0$, $x \in \mathbb{R}$

$$\rho_t + (\rho w)_x = 0 \tag{9}$$

$$\begin{aligned}\rho q(w)w_t + \rho q(w)ww_x + P'(\rho)\rho_x = (\mu(\rho)g'(w)w_x)_x \\ - \rho f(w)\end{aligned} \tag{10}$$

with constraints $\rho(t,x) \in [0, R)$, $w(t,x) \in (-1, b)$ for $t > 0$, $x \in \mathbb{R}$, where $R > 1$, $b > 0$ are constants, $g \in C^1(\mathbb{R})$ is an increasing function with $g'(w) > 0$ for all $w \in (-1, b)$, $f : \mathbb{R} \to \mathbb{R}$ with $f(0) = 0$ is a C^1 function with $wf(w) > 0$ for all $w \neq 0$, and

$$q(w) = (1+b)^2 \frac{2b + (b-1)w}{2(b-w)^2(1+w)^2} \text{ for all } w \in (-1, b) \tag{11}$$

Moreover, the functions $\mu : [0, R) \to \mathbb{R}_+$, $P : [0, R) \to \mathbb{R}_+$ are $C^1([0, R))$ and satisfy the following properties:

$$\lim_{\rho \to R^-} P(\rho) = +\infty \tag{12}$$

$$\begin{aligned}&\mu(\rho) = 0,\ \ P(\rho) = 0 \text{ for all } \rho \in [0, 1], \text{ and} \\ &\mu(\rho) > 0,\ P(\rho) > 0 \text{ for all } \rho \in (1, R).\end{aligned} \tag{13}$$

Model (9), (10) is studied under the following conditions for all $t \geq 0$:

$$\lim_{x \to \pm\infty} \rho(t,x) = 0 \tag{14}$$

$$\lim_{x \to \pm\infty} w(t,x) = 0 \tag{15}$$

$$\int_{-\infty}^{+\infty} \rho(t,x)dx < +\infty \tag{16}$$

If the parameters of the cruise controller that is applied to the vehicles are selected in such a way that

$$g(w) = w \text{ for all } w \in (-1, b) \tag{17}$$

$$P'(\rho) = k\rho^{-1}\mu(\rho) \tag{18}$$

$$\begin{aligned}\beta(w) = \int_0^w q(s)ds = \frac{b+1}{2}\Bigg[\frac{w(b+1)}{(w+1)(b-w)} \\ + \ln\left(\frac{b(w+1)}{b-w}\right)\Bigg], \text{ for all } w \in (-1, b)\end{aligned} \tag{19}$$

$$f(w) = k\beta(w) \tag{20}$$

where $k > 0$ is a constant and the function $\mu : [0, R) \to \mathbb{R}_+$ satisfies

$$\lim_{\rho \to R^-} \mu(\rho) = +\infty \tag{21}$$

then using definitions (17), (18), (19), and (20), the resulting PDE model (9), (10), becomes

$$\rho_t + (\rho w)_x = 0 \tag{22}$$

$$\rho\beta'(w)w_t + \rho\beta'(w)ww_x + k\rho^{-1}\mu(\rho)\rho_x = (\mu(\rho)w_x)_x - k\rho\beta(w) \tag{23}$$

with $t > 0$, $x \in \mathbb{R}$.

Remark: Definitions (17), (20), (18), (21), in addition to simplifying the original model (9), (10), have important implications. Definition (17) is met in real fluid flows in non-porous media, see [1], while condition (21) for the dynamic viscosity makes the fluid behave like a solid when density tends to the maximum density R.

Assume now that $\rho(t, x) > 0$ for $t > 0$, $x \in \mathbb{R}$ and that (14), (15), and (16) hold. Define

$$\varphi(t, x) = \rho(t, x)\beta\left(w(t, x)\right) + \rho^{-1}(t, x)\mu(\rho(t, x))\rho_x(t, x) \quad \text{for all } t > 0 \text{ and } x \in \mathbb{R} \tag{24}$$

where $\beta(w)$ is given in (19). Equations (22), (23) and definition (24) imply the following equation for $t > 0$, $x \in \mathbb{R}$:

$$\varphi_t + (w\varphi)_x = -k\varphi. \tag{25}$$

Next, define

$$g(t, x) = \frac{\varphi(t, x)}{\rho(t, x)} \exp(kt), \text{ for all } t > 0 \text{ and } x \in \mathbb{R}. \tag{26}$$

Thus, we get from (22), (23), (25), and (26) that

$$g_t + wg_x = 0. \tag{27}$$

It follows from (27) that $\|g[t]\|_\infty \leq \|g[0]\|_\infty$ for all $t \geq 0$, which, combined with (26), implies that the following estimate holds:

$$\left\| \frac{\varphi[t]}{\rho[t]} \right\|_\infty \leq \exp(-kt) \left\| \frac{\varphi[0]}{\rho[0]} \right\|_\infty \text{ for all } t \geq 0. \tag{28}$$

Inequality (28) and definition (24) imply that for all $x \in \mathbb{R}$:

$$\lim_{t \to +\infty} \left(\beta\left(w(t, x)\right) + \rho^{-2}(t, x)\mu(\rho(t, x))\rho_x(t, x)\right) = 0. \tag{29}$$

Since $\beta\left((-1, b)\right) = \mathbb{R}$, we can define the inverse function $h : \mathbb{R} \to (-1, b)$ with $h(0) = 0$ and $h'(s) > 0$ for all $s \in \mathbb{R}$. Thus, we get from (29) for all $x \in \mathbb{R}$:

$$\lim_{t \to +\infty} \left(w(t, x) - h\left(-\rho^{-2}(t, x)\mu(\rho(t, x))\rho_x(t, x)\right)\right) = 0. \tag{30}$$

Inequality (28) and equation (30) imply that the manifold $w(t, x) = h\left(-\rho^{-2}(t, x)\mu(\rho(t, x))\rho_x(t, x)\right)$ is exponentially attracting.

Consequently, the solutions of (9), (10) are approximated by the solutions of the following PDE that holds for $t > 0$, $x \in \mathbb{R}$

$$\rho_t + \left(\rho h\left(-\kappa(\rho)\rho_x\right)\right)_x = 0$$

where

$$\kappa\left(\rho\right) := \rho^{-2}\mu(\rho) \text{ for } \rho \in (0, R). \tag{31}$$

Notice that from definition (31) and (13), (21), it follows that $\kappa(\rho) = 0$ for all $\rho \in (0, 1]$ and $\kappa(\rho) > 0$ for all $\rho \in (1, R)$.

B. The Model and its Properties

Motivated by the analysis of the previous section, we study hereafter the following model and its properties

$$\rho_t + \left(\rho h\left(-\kappa(\rho)\rho_x\right)\right)_x = 0, t > 0, x \in \mathbb{R} \tag{32}$$

where $\kappa \in C^1\left([0, R); \mathbb{R}_+\right)$ with $\kappa(\rho) = 0$ for all $\rho \in [0, 1]$ and $\kappa(\rho) > 0$ for all $\rho \in (1, R)$, and $h \in C^1\left(\mathbb{R}; (-1, b)\right)$ with $h' \in L^\infty\left(\mathbb{R}\right)$ and satisfies $h(0) = 0$ and $h'(s) > 0$ for all $s \in \mathbb{R}$. The PDE (32) is studied under the condition:

$$\lim_{x \to \pm\infty} \left(\rho(t, x)\right) = 0, \text{ for all } t > 0 \tag{33}$$

with state constraint $\rho(t, x) \in [0, R)$ for all $t > 0$ and $x \in \mathbb{R}$, and $\int_{-\infty}^{+\infty} \rho(t, x)dx < +\infty$ for all $t \geq 0$.

We notice that :

• There are infinite equilibrium points, namely the points where $\rho(x) \leq 1$ for all $x \in \mathbb{R}$.

• The nonlinear PDE (32) is not hyperbolic and is not parabolic. When $\rho(t, x) \leq 1$, we get $\rho_t(t, x) = 0$ (a zero-speed hyperbolic PDE) with the propagation speed being zero; and when $\rho(t, x) > 1$, we get the following equation

$$\rho_t + h\left(-\kappa(\rho)\rho_x\right)\rho_x - \rho h'\left(-\kappa(\rho)\rho_x\right)\kappa'(\rho)\rho_x^2 = \rho h'\left(-\kappa(\rho)\rho_x\right)\kappa(\rho)\rho_{xx} \tag{34}$$

• The PDE (32) (see also (34)) is a nonlinear heat equation with the diffusion coefficient depending on both the density ρ and the spatial derivative of the density ρ_x.

Define the set

$$X = \Big\{\rho \in L^1\left(\mathbb{R}\right) \cap L^\infty\left(\mathbb{R}\right) : \inf_{x \in \mathbb{R}} \left(\rho(x)\right) = 0, \sup_{x \in \mathbb{R}} \left(\rho(x)\right) < R, \lim_{x \to \pm\infty} \left(\rho(x)\right) = 0\Big\}. \tag{35}$$

Using (32), it can be shown that for every classical solution $\rho \in C^1\left(\mathbb{R}_+ \times \mathbb{R}; [0, R)\right) \cap C^2\left((0, +\infty) \times \mathbb{R}\right)$ of (32), (33) with $\rho[t] \in X$ for all $t \geq 0$, it holds that

$$\dot{m}(t) = 0 \text{ for } t > 0 \tag{36}$$

where $m(t)$ is the total mass

$$m(t) = \int_{-\infty}^{+\infty} \rho(t, x)dx. \tag{37}$$

Therefore, the total mass remains constant. The fact that mass is conserved is of great importance, since it characterizes physically admissible solutions.

For any classical solution $\rho \in C^1(\mathbb{R}_+ \times \mathbb{R}; [0, R)) \cap C^2((0, +\infty) \times \mathbb{R})$ of (32), (33) with $\rho[t] \in X$ for all $t \geq 0$, we can define the following functionals

$$E_1(t) = \int_{-\infty}^{+\infty} \rho(t,x) H\left(-\kappa(\rho(t,x))\rho_x(t,x)\right) dx \quad (38)$$

$$E_2(t) = \int_{-\infty}^{+\infty} Q(\rho(t,x)) dx \quad (39)$$

where

$$H(w) := \int_0^w h(s) ds \text{ for all } w \in (-1, b) \quad (40)$$

$$Q(\rho) := \int_1^\rho (\rho - \tau)\, \kappa(\tau)\, d\tau \text{ for all } \rho \in [0, R). \quad (41)$$

The above functionals are inspired by the mechanical energy of the original model (22), (23), with the functional E_1 in (38) expressing the kinetic energy and the functional E_2 in (39) expressing the potential energy. A direct consequence of (32) and the functionals defined by (38) and (39) are the following inequalities that hold for all classical solutions $\rho \in C^1(\mathbb{R}_+ \times \mathbb{R}; [0, R)) \cap C^2((0, +\infty) \times \mathbb{R})$ of (32), (33) with $\rho[t] \in X$ for all $t \geq 0$:

$$\begin{aligned} &\dot{E}_1(t) = \\ &-\int_{-\infty}^{+\infty} \rho^2(t,x) \kappa(\rho(t,x)) \left(h\left(-\kappa(\rho(t,x))\rho_x(t,x)\right)\right)_x^2 dx \leq 0, \\ &\text{for } t > 0 \end{aligned} \quad (42)$$

$$\begin{aligned} &\dot{E}_2(t) = \\ &\int_{-\infty}^{+\infty} \rho(t,x) \kappa(\rho(t,x)) \rho_x(t,x) h\left(-\kappa(\rho(t,x))\rho_x(t,x)\right) dx \leq 0, \\ &\text{for } t > 0. \end{aligned} \quad (43)$$

Inequalities (42), (43) show us that both functionals (38), (39) are decreasing along classical solutions of (32). Inequality (43) gives an entropy-like condition that characterize physically meaningful solutions, see [7], [24].

Let the initial condition

$$\rho[0] = \rho_0 \in X \quad (44)$$

be given.

III. A NUMERICAL SCHEME AND ITS PROPERTIES

Using finite-differences for (32) with time-step $\delta t > 0$ and spatial discretization $\delta x > 0$, we next study the following explicit numerical scheme

$$\rho_i^+ = \rho_i + \frac{\delta t}{\delta x}\left(G_{i-1} - G_i\right), i \in \mathbb{Z} \quad (45)$$

where

$$G_i = \rho_i w_i = \rho_i h\left(-q_i\right), i \in \mathbb{Z} \quad (46)$$

$$q_i = -\beta(w_i) = \frac{Q'(\rho_{i+1}) - Q'(\rho_i)}{\delta x}, i \in \mathbb{Z} \quad (47)$$

with $\rho_i \in [0, R)$ for $i \in \mathbb{Z}$ and $M = \sup_{i \in \mathbb{Z}} (\rho_i) < R$ be given and $\beta : (-1, b) \to \mathbb{R}$ being the inverse of $h : \mathbb{R} \to (-1, b)$. Here ρ_i is the numerical value of density at the point $x = i\delta x$ and at time $t \geq 0$, while ρ_i^+ is the numerical value of density at the point $x = i\delta x$ and at time $t + \delta t$. The numerical scheme (45)-(47) is a first-order accurate discretization and is appropriately designed to respect the entropy-like condition (43), for sufficiently small time-step δt, and to satisfy certain very important properties, such as conservation of mass, that are discussed in detail below.

A direct consequence of the discretization (45)-(47) above, is that the mass $m(t)$ remains constant showing that the numerical scheme is conservative, see [18]. Indeed, we have

Proposition 1: *For every sequence $\rho_i \in [0, R)$, $i \in \mathbb{Z}$ with $\sum_{i \in \mathbb{Z}} \rho_i < +\infty$, it holds that $\sum_{i \in \mathbb{Z}} \rho_i^+ = \sum_{i \in \mathbb{Z}} \rho_i$.*

Notice that Proposition 1 implies that $\lim_{t \to \pm\infty} \rho_i^+ = \inf_{i \in \mathbb{Z}} \rho_i^+ = 0$ for every sequence $\rho_i \in [0, R)$, $i \in \mathbb{Z}$ with $\sum_{i \in \mathbb{Z}} \rho_i < +\infty$. To complete the discretization of model (32), the above scheme has to be supplemented with a suitable time-step for certain properties to be preserved. In the following propositions, we obtain an upper bound on the time discretization step δt, for a given space discretization δx, which guarantees that the functional E_2 defined by (39) is non-increasing (in a discretized sense). In particular, it is proved that, in addition to the numerical scheme being conservative, it also respects the entropy condition (43).

Proposition 2: *Define $f(\delta t) = \delta x \sum_{i \in \mathbb{Z}} Q(\rho_i^+)$ for all $\delta t \geq 0$. Then $\frac{df}{d\delta t}(0) = \delta x \sum_{i \in \mathbb{Z}} \rho_i q_i h\left(-q_i\right) \leq 0$.*

Proposition 3: *Suppose that $1 \geq \frac{\delta t}{\delta x}\left(b + 2\frac{M\|h'\|_\infty}{\delta x} \max_{0 \leq \rho \leq M} (\kappa(\rho))\right)$. Then $\rho_i^+ \in [0, M]$ for all $i \in \mathbb{Z}$, where $M = \sup_{i \in \mathbb{Z}} (\rho_i) < R$.*

For given δx, the bound on the time-step provided in Proposition 3, establishes that ρ_i is non-negative and remains bounded by $M = \sup_{i \in \mathbb{Z}} (\rho_i) < R$ for all $i \in \mathbb{Z}$. It should be noted that the condition on the time-step is an analogous nonlinear version of the well-known *Courant-Friedrichs-Lewy (CFL)* condition, see [26]. Finally, under the same bounds on time-step δt, as in Proposition 3, it is shown next that the functional E_2 in (39) is non-increasing.

Proposition 5: *Suppose that $1 \geq \frac{\delta t}{\delta x}\left(b + 2\frac{M\|h'\|_\infty}{\delta x} \max_{0 \leq \rho \leq M} (\kappa(\rho))\right)$. Then*

$$\begin{aligned} &\textstyle\sum_{i \in \mathbb{Z}} Q(\rho_i^+) \leq \sum_{i \in \mathbb{Z}} Q(\rho_i) \\ &+\delta t \left(1 - \delta t \frac{4M\|h'\|_\infty}{(\delta x)^2} \max_{0 \leq \rho \leq M} (\kappa(\rho))\right) \sum_{i \in \mathbb{Z}} \rho_i q_i h\left(-q_i\right) \\ &= \textstyle\sum_{i \in \mathbb{Z}} Q(\rho_i) \\ &-\delta t \left(1 - \delta t \frac{4M\|h'\|_\infty}{(\delta x)^2} \max_{0 \leq \rho \leq M} (\kappa(\rho))\right) \sum_{i \in \mathbb{Z}} \rho_i w_i \beta\left(w_i\right) \\ &\leq \textstyle\sum_{i \in \mathbb{Z}} Q(\rho_i) \end{aligned} \quad (48)$$

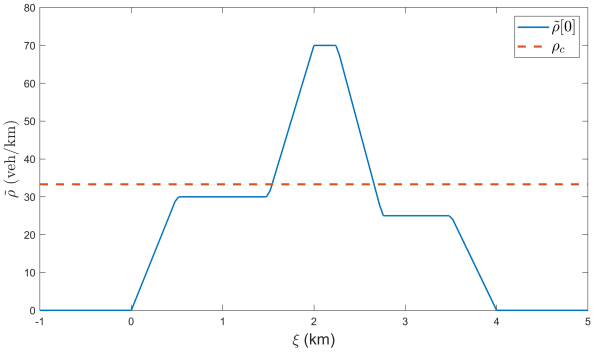

Fig. 1. Initial density $\tilde{\rho}_0(\xi)$.

IV. NUMERICAL EXPERIMENTS

In this section, we consider a traffic scenario and compare the density and flow of (32) with one of the most well-known traffic flow models for human drivers, the so-called LWR model ([16], [21])

$$\tilde{\rho}_\tau + (\tilde{\rho}\tilde{v})_\xi = 0, \tau > 0, \xi \in \mathbb{R} \tag{49}$$

with the speed $\tilde{v}$ given by

$$\tilde{v}(\tau, \xi) = v_{\max} \exp\left(-\frac{1}{a}\left(\frac{\tilde{\rho}(\tau, \xi)}{\rho_c}\right)^a\right) \tag{50}$$

where $v_{\max} > 0$ is the maximum speed (free-flow speed), ρ_c is the critical density, and $a > 0$ is a parameter.

Our model (32), in the original variables $\tau > 0$, $\xi \in \mathbb{R}$, is given by equation (49) with the speed $\tilde{v}$ defined by

$$\tilde{v}(t, \xi) = v^*\left(1 + h\left(-\mu\left(\frac{\tilde{\rho}(\tau, \xi)}{\bar{\rho}}\right)\frac{\tilde{\rho}_\xi(\tau, \xi)\bar{\rho}}{\tilde{\rho}^2(\tau, \xi)}\right)\right) \tag{51}$$

(recall the transformation $\xi = rx + v^*\tau$, $x \in \mathbb{R}$ and the quantities $\tau = \frac{r}{v^*}t$, $w = \frac{\tilde{v}-v^*}{v^*}$, $\rho = \frac{\tilde{\rho}}{\bar{\rho}}$, with $r = 1$), where

$$h(s) = \beta^{-1}(s), s \in \mathbb{R} \tag{52}$$

with $\beta(w)$ defined by (19), and $\mu(\rho)$ given by

$$\mu(\rho) = \begin{cases} 0 & , 0 \le \rho \le 1 \\ c\frac{(\rho-1)^2}{R-\rho} & , 1 < \rho < R \end{cases} \tag{53}$$

where $c > 0$ is parameter. Therefore, (49), (51), is a first-order automated vehicle model (AV model).

We consider a single-lane motorway with $v_{\max} = 110$ (km/h), $\rho_{\max} = 180$ (veh/km), $\rho_c = 33.3$ (veh/km), and $a = 2.34$ that are selected based on real data from a part of the Amsterdam A10 motorway (without on-ramps and off-ramps), see [4]. In this scenario, we assume that the initial density on the road is characterized by a congestion belt in the interval $[1.5\,, 2.75\,]$ (km) as shown in Fig. 1 with $\tilde{\rho}_0(\xi) = 0$ for $\xi < 0$ and $\xi > 0$. Note also that outside the congested area, the density is below the critical density ρ_c.

For the parameters of the AV model (49), (51), we select the speed set-point $v^* = 70$ (km/h) (significantly smaller than the speed limit), the viscosity constant $c = 40$, interaction density $\bar{\rho} = 31$ and recall that the quantities R and b are given by $R = \frac{\rho_{max}}{\bar{\rho}} > 1$ and $b = \frac{v_{max}-v^*}{v^*}$, respectively. For the LWR model, we consider the interval $\xi \in [0, 120]$ and

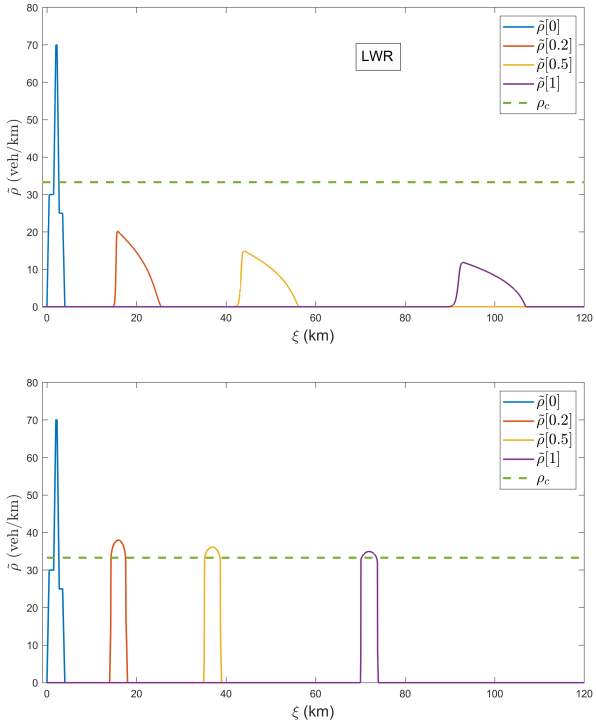

Fig. 2. Density profiles for the LWR (top), and density profiles of AV model (bottom).

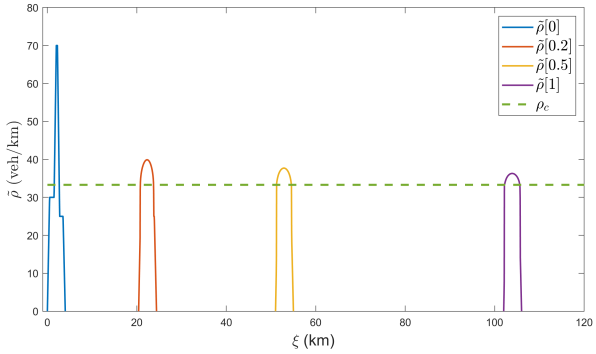

Fig. 3. Density profiles of the AV model with $v^\star = 102$ (km/h).

use Godunov's method to obtain its solution. The density profiles for both models over a simulation time of $1h$ are shown in Fig. 2.

Fig. 2 shows that the density of both models dissipates along the road. However, for the LWR model the dissipation is much stronger and the density is spread over a large road interval for increasing $\tau > 0$. More specifically, for $\tau = 1$ (h), the density is non-zero over the interval $[90, 106]$ (km), which implies that the vehicles retain large inter-vehicle distances while the maximum density is equal to $\max_{\xi\in[90,106]}(\tilde{\rho}[1]) = 11.8$ (veh/km). On the other hand, for the AV model, the density dissipates at a lower rate but the vehicles remain in a 4km stretch of the road ($\xi \in [70\,, 74]$ (km), since the desired speed is $v^* = 70$ (km/h)), as was the case in the initial density, and with maximum density $\max_{\xi\in[70,74]}(\tilde{\rho}[1]) = 34.94$ (veh/km) (near the critical density ρ_c). Note also that the density for the AV model converges towards an equilibrium where $\tilde{v}(\xi) \equiv v^*$ and $\tilde{\rho}(\xi) \le \bar{\rho} < \rho_c$.

	AV model (49), (51) with $v^* = 70$ (km/h)	AV model (49), (51) with $v^* = 102$ (km/h)	LWR
Mean Flow	2232 (veh/h)	3201 (veh/h)	926 (veh/h)

TABLE I
MEAN FLOW

Moreover, we also consider the case where the speed set-point is equal to the free-flow speed $v^* = v_f = 102$ (km/h). The density profiles of the AV model with $v^* = 102$ (km/h) are shown in Fig. 3. Note that when vehicles are moving with free-flow speed $v^* = 102$ (km/h), the overall travel time is higher with the AV model, since, for $\tau = 1$ (h), vehicles are in the interval $(102, 106)$ (km), whereas with the LWR, vehicles are in the interval $(90, 106)$ (km), compare with Fig. 2 (top). The latter implies that the flow $q = \tilde{\rho}\tilde{v}$ of model AV model is much higher than the flow of the LWR model, or equivalently, vehicles equipped with the cruise controllers proposed in [11] will retain smaller inter-vehicle distances (higher density) than human-driven vehicle. To compare the mean flow for each model, we define

$$\text{Mean Flow } = \frac{1}{T}\int_0^T \int_{a(t)}^{b(t)} \frac{\tilde{\rho}(t,x)\tilde{v}(t,x)}{b(t)-a(t)} dxdt$$

where $T > 0$ denotes the maximum time and $[a(\tau), b(\tau)]$ denotes the interval where $\tilde{\rho}(\tau, \xi) \neq 0$ for $\xi \in [a(\tau), b(\tau)]$ at each time instant $\tau \geq 0$. We consider the cases: (i) $v^* = 70$ (km/h) - the speed set-point is much lower than the free-flow speed; and (ii) $v^* = 102$ (km/h) - the speed set-point is equal to the free flow speed v_f. The mean flow for both models and $T = 1$ (h) is shown in Table I. In both cases, the mean flow for the AV model is much higher than the mean flow of the LWR. In particular, when the vehicles are moving with free-flow speed, the mean flow of the AV model is 346% higher than the mean flow of the LWR model.

V. CONCLUSIONS

We have studied the performance of a class of cruise-controllers for automated vehicles on a macroscopic scale. We have shown that the solution of the corresponding second-order macroscopic model can be approximated by the solution of a nonlinear heat-type equation. A conservative finite-difference scheme was proposed that respects the corresponding entropy conditions. Finally, to evaluate the performance of cruise-controlled vehicles, a traffic simulation scenario and a comparison with the Lighthill-Witham-Richards (LWR) model were given.

REFERENCES

[1] Aronson, D. G., "The Porous Medium Equation", in: A. Fasano, M. Primicerio (eds) *Nonlinear Diffusion Problems*, Lecture Notes in Mathematics, 1224, Springer, 1986, 1-46.

[2] Aw, A. and M. Rascle, "Resurrection of Second-Order Models of Traffic Flow", *SIAM Journal on Applied Mathematics,* 60, 2000, 916–938.

[3] Buckmire, R., McMurtry, K. and Mickens, R.E., "Numerical Studies of a Nonlinear Heat Equation with Square Root Reaction Term", *Numerical Methods for Partial Differential Equations*, 25, 2009, 598-609.

[4] Carlson, R. C., I. Papamichail, M. Papageorgiou, and A. Messmer, "Optimal Mainstream Traffic Flow Control of Large-Scale Motorway Networks", *Transportation Research Part C: Emerging Technologies*, 18, 193-212, 2010.

[5] Cho C. H., "On the Finite Difference Approximation for Blow-up Solutions of the Porous Medium Equation with a Source", *Applied Numerical Mathematics,* 65, 2013, 1-26.

[6] Christou, M.A., C. Sophocleous, and C.I. Christov, "Numerical Investigation of the Nonlinear Heat Diffusion Equation with High Nonlinearity on the Boundary", *Applied Mathematics and Computation*, 201, 2008, 729-738.

[7] Dafermos, C. M., *Hyperbolic Conservation Laws in Continuum Physics, Dynamical Systemsand Differential Equations*, Springer, 2010.

[8] Edelstein, RM and Govinder, KS., "On the Method of Preliminary Group Classification Applied to the Nonlinear Heat Equation $u_t = f(x, u_x)u_{xx}+g(x, u_x)$", *Mathematical Methods in Applied Sciences*, 43, 2020, 5927- 5940.

[9] Goatin, P. and N. Laurent-Brouty, "The Zero Relaxation Limit for the Aw–Rascle–Zhang Traffic Flow Model", *Zeitschrift für angewandte Mathematik und Physik,*70, 2019.

[10] Jovanovic B.S., P.P. Matus, and V.S. Shchehlik, "The Estimates of Accuracy of Difference Schemes for the Nonlinear Heat Equation with Weak Solution", *Mathematical Modelling and Analysis,* 5, 2000, 86-96.

[11] Karafyllis I., D. Theodosis, and M. Papageorgiou, "Constructing Artificial Traffic Fluids by Designing Cruise Controllers", *Systems & Control Letters*, 167, 2022.

[12] Karafyllis, I. and M. Krstic, "Global Stabilization of Compressible Flow Between Two Moving Pistons", *SIAM Journal on Control and Optimization*, 60, 2022, 1117-1142.

[13] Karafyllis I. and M. Krstic, "Spill-Free Transfer and Stabilization of Viscous Liquid," in *IEEE Transactions on Automatic Control*, 67, 4585-4597, 2022.

[14] Ladyzhenskaya, O. A., V. A. Solonnikov and N. N. Ural'ceva, *Linear and Quasilinear Equations of Parabolic Type*, Translations of AMS, Vol. 23, 1968.

[15] Ladyzhenskaya, O. A., "New Equations for the Description of the Motions of Viscous Incompressible Fluids, and Global Solvability for their Boundary Value Problems", *Boundary Value Problems of Mathematical Physics,* Part 5, Trudy Matematicheskogo Instituta imeni V.A. Steklova, 102, 1967, 85–104 and Proceedings of the Steklov Institute of Mathematics, 102, 1967, 95-118.

[16] Lighthill, M. H. and G. B. Whitham, "On Kinematic Waves II: A Theory of Traffic Flow on Long Crowded Roads", *Proceedings of the Royal Society A*, 229, 1955, 317–345.

[17] Lions, P.-L., *Mathematical Topics in Fluid Dynamics,* Vol.2, Compressible Models, Oxford Science Publication, Oxford, 1998.

[18] Leveque, R.J., *Numerical Methods for Conservation Laws,* Birkhäuser, Basel, 1992.

[19] N'Gohisse, F.K., and T.K. Boni, "Numerical Blow-up for a Nonlinear Heat Equation", *Acta Mathematica Sinica,-English Series,* 27, 2011, 845–862.

[20] Popovych R. O. and N. M. Ivanova, "Potential Equivalence Transformations for Nonlinear Diffusion-Convection Equations", *Journal of Physics A: Mathematical and General* , 38, 2005, 3145—3155.

[21] Richards, P. I., "Shock Waves on the Highway", *Operations Research*, 4, 1956, 42–51.

[22] Rincon, M.A., J. Límaco, and I-Shih. Liu, "A Nonlinear Heat Equation with Temperature-dependent Parameters", *Mathematical Physics Electronic Journal [electronic only]* 12, 2006, 21.

[23] Rodriguez A., J. L. Vazquez, "Non-Uniqueness of Solutions of Nonlinear Heat Equations of Fast Diffusion Type", *Annales de l'Institut Henri Poincaré C, Analyse non linéaire,* 12, 1995, 173-200,

[24] Smoller, J., *Shock Waves and Reaction-Diffusion Equations*, 2^{nd} Edition, Springer-Verlag, New York, 1994.

[25] Theodosis, D., I. Karafyllis, G. Titakis, I. Papamichail and M. Papageorgiou, "A Nonlinear Heat Equation Arising from Automated-Vehicle Traffic Flow Models", submitted to the Journal of Computational and Applied Mathematics (see arXiv:2210.04321 [math.NA]).

[26] Thomas J., *Numerical Partial Differential Equations: Finite Difference Methods*, Springer, 1995.

[27] Zhang, H. M., "A Non-Equilibrium Traffic Model Devoid of Gas-like Behavior", *Transportation Research Part B*, 36, 2002, 275–290.